

## Temporal analysis of E2 transcriptional induction of PTP and MKP and downregulation of IGF-I pathway key components in the mouse uterus

Mahinè Ivanga, Yvan Labrie, Ezequiel Calvo, Pascal Belleau, Céline Martel, Van Luu-The, Jean Morissette, Fernand Labrie, and Francine Durocher

Oncology and Molecular Endocrinology Research Center, Centre Hospitalier de l'Université Laval (CHUL) Research Center, Centre Hospitalier Universitaire de Québec (CHUQ), Department of Anatomy and Physiology, Laval University, Québec, Canada

Submitted 24 November 2005; accepted in final form 21 November 2006

**Ivanga M, Labrie Y, Calvo E, Belleau P, Martel C, Luu-The V, Morissette J, Labrie F, Durocher F.** Temporal analysis of E2 transcriptional induction of PTP and MKP and downregulation of IGF-I pathway key components in the mouse uterus. *Physiol Genomics* 29: 13–23, 2007; doi:10.1152/physiolgenomics.00291.2005.—17 $\beta$ -Estradiol (E2) is well known to be associated with uterine cancer, endometriosis, and leiomyomas. Although insulin-like growth factor I (IGF-I) has been identified as a mediator of the uterotrophic effect of E2 in several studies, this mechanism is still not well understood. In the present study, identification of the genes modulated by a physiological dose of E2, in the uterus, has been done in ovariectomized mice using Affymetrix microarrays. The E2-induced genomic profile shows that multiple genes belonging to the IGF-I pathway are affected after exposure to E2. Two phases of regulation could be identified. First, from 0 to 6 h, the expression of genes involved in the cell cycle, growth factors, protein tyrosine phosphatases, and MAPK phosphatases is quickly upregulated by E2, while IGF-I receptor and several genes of the MAPK and phosphatidylinositol 3-kinase pathways are downregulated. Later, i.e., from 6 to 24 h, transporters and peptidases/proteases are stimulated, whereas defense-related genes are differentially regulated by E2. Finally, cytoarchitectural genes are modulated later. The present data show that a physiological dose of E2 induces, within 24 h, a series of transcriptional events that promote the uterotrophic effect. Among these, the E2-mediated activation of the IGF-I pathway seems to play a pivotal role in the uterotrophic effect. Furthermore, the protein tyrosine phosphatases and MAPK phosphatases are likely to modulate the estrogenic uterotrophic action by targeting, at different steps, the IGF-I pathway.

17 $\beta$ -estradiol; 17 $\beta$ -estradiol modulation; ovariectomized mice; oligonucleotide microarray; protein tyrosine phosphatase

IN MAMMALS, THE UTERUS of a mature female undergoes multiple changes during the estrous cycle that reflect modifications of the uterine endometrium in continuous preparation for embryo implantation. Since the majority of cycles are not associated with conception, they often lead to endometrial degeneration and menstrual bleeding. The endometrium thus exhibits a cyclic pattern of growth, regression, disruption, bleeding, and regeneration throughout reproductive life. These changes are mainly under the control of estrogens, progesterone, and androgens. Disregulation of the uterine vasculature has been found to accompany different sex steroid disturbances (28).

17 $\beta$ -Estradiol (E2) is well known to play the key role in mammalian endometrial physiology, since the proliferation of endometrial cells and the extension of spiral vessels that occur

during the proliferative phase of the menstrual cycle are controlled by E2 (20, 46). Estrogen is also frequently associated with endometrial cancer, which comprises two subtypes: endometrioid carcinomas (type I) related to estrogen exposure and nonendometrioid carcinomas (type II), which are independent of E2 action (16). Type I cancers are characterized by mutation or upregulation of the expression of genes involved in cell cycle/intracellular trafficking, structural/cytoskeleton, and peptidases/proteases functions. Defects in DNA repair and a near-diploid karyotype are also observed.

Type II cancers often display mutations or amplification of cell cycle- and intracellular trafficking-related genes and growth factor-related genes (37, 41, 56). However, the majority of cases of endometrial cancers lack mutations in the family of genes cited above, thus suggesting that the molecular pathogenesis of endometrial cancer is not well understood. Furthermore, dysregulation of specific groups of genes leads to numerous physiological disorders, namely, endometriosis (32), excessive bleeding (8), and cell aberrant growth (28, 32).

Therefore, to identify key genes that could be potentially implicated in uterine cancer susceptibility, this study focused particularly on the E2 modulation of the insulin-like growth factor I (IGF-I) signal transduction pathway, which involves the action of insulin-like growth factor binding proteins (IGFBPs) and the regulation of protein tyrosine phosphatases (PTPs) and MAPK phosphatases (MKPs).

IGF-I is defined as an estromedin transcriptionally activated by E2. IGF-I exerts also a strong influence on cell proliferation and differentiation (59) and is a potent inhibitor of apoptosis in human osteoblasts (33). The action of IGF-I is mainly mediated through the IGF-I receptor (IGF-IR), which is found throughout the uterus (myometrium, epithelium, and stroma), where cells proliferate in response to added IGF-I (63). IGF-I signal transduction involves the activation of several intracellular signaling pathways, including the Ras/Raf/MAPK and the phosphatidylinositol 3-kinase (PI3K) pathways (68). Furthermore, IGF-I is seen as an important mediator of the E2 uterotrophic action in mouse (42), as IGF-I-deficient female mice are infertile and display uterine hypoplasia (3), thus suggesting that the IGF-I action is an important determinant of uterine function. Interestingly, it has been indicated that, in the uterus, E2 can rapidly stimulate a sustained increase in the tyrosine phosphorylation of IGF-IR and insulin receptor substrate-1 (IRS-1) (55).

In contrast, PTPs can modulate protein kinase activity either directly or by controlling the phosphorylation state of protein kinase substrates. Dysregulation of PTP functions induces an

Article published online before print. See web site for date of publication (<http://physiolgenomics.physiology.org>).

Address for reprint requests and other correspondence: F. Durocher, CREMO, CHUL Research Center, 2705 Laurier Blvd., T2-53, Québec (Québec), Canada G1V4G2 (e-mail: Francine.Durocher@crchul.ulaval.ca).

aberrant tyrosine phosphorylation and contributes to the development of many human diseases (73). For example, it has been shown that PTP1B can inhibit the tyrosine activity of the full-length IGF-IR in mammalian cells (7) and is also able to inhibit hormone-induced phosphorylation of the insulin receptor by specifically targeting the pTyr-1162 residue on its activation segment (58). The MKPs are dual-specificity phosphatases that inactivate MAPKs by specifically dephosphorylating their pTyr and pThr residues, and whose expression is in turn transcriptionally regulated by MAPKs. It has also been demonstrated that the growth factor-stimulating network containing MAPK1/2 follows a two-states model, which is MKP concentration dependent (5).

Even if several genes are known to be E2 responsive, the mechanisms regulating their temporal modulation remain poorly understood, and previous studies have mainly been performed on cultured cells. Microarray analysis provides a powerful tool for analyzing complex biological systems, allowing the identification of gene expression patterns. However, other studies of the rodent uterine genomic profiles have been performed using supraphysiological doses of E2 and/or less time points following E2 exposure (26, 27, 39, 70). Hence, in this study, to better understand the *in vivo* events triggered by a physiological dose of E2 at the transcriptional level in the uterus, time course uterine gene expression profiles were examined using oligonucleotide microarray analysis and further validated by quantitative real-time PCR (Q-RT-PCR). Our data provide new insights into how E2 finely modulates the IGF-I signal effect in uterine cells and could potentially lead to the identification of cancer susceptibility genes in uterus or other E2-dependent tissues like breast or ovary.

## MATERIALS AND METHODS

### *Animals and Treatment*

Ten-week-old female C57BL6 mice were received from Charles River (St-Constant, QC, Canada) and were allowed to acclimate for 3 wk. The animals were housed individually in an environmentally controlled room (temperature,  $22 \pm 3^\circ\text{C}$ ; humidity,  $50 \pm 20\%$ ; 12:12-h light-dark cycles, lights on at 0715). The mice had free access to tap water and a certified rodent feed [Lab Diet 5002 (pellet); Ralston Purina, St Louis, MO]. The experiment was conducted in an animal facility approved by the Canadian Council on Animal Care (CCAC) and the Association for Assessment and Accreditation of Laboratory Animal Care. The study was submitted and approved by the CPA-CHUQ ethical committee and was performed in accordance with the CCAC Guide for Care and Use of Experimental Animals.

Animals, weighing between 20 and 24 g, were randomized according to their body weights and were assigned to 6 groups of 14 animals each as follows: *group 1*, gonadectomized (GDX) control; *groups 2–6*, GDX +  $17\beta$ -estradiol (E2; 0.05  $\mu\text{g}/\text{mouse}$ ). On *day 1* of the study, animals were bilaterally ovariectomized (GDX) under isoflurane anesthesia. Before the necropsy, performed on *day 8* of the study, mice received a single subcutaneous injection (0.2 ml/mouse) of the vehicle alone (5% ethanol-0.4% methylcellulose; *group 1*) or E2 (*groups 2–6*). The injection of vehicle was performed 24 h before the necropsy for animals in *group 1*, while E2 was injected 1 h (*group 2*), 3 h (*group 3*), 6 h (*group 4*), 12 h (*group 5*), or 24 h (*group 6*) before the necropsy.

On *day 8* of the study, mice under isoflurane anesthesia were exsanguinated at the abdominal aorta followed by cervical dislocation. The uterus was collected and rapidly frozen in liquid nitrogen. Tissues were pooled and kept at  $-80^\circ\text{C}$  until RNA extraction. According to the treatment, the temporal mRNA changes of 12,000 genes were

analyzed by Affymetrix oligonucleotide microarray analysis (MG-U74 v2).

### *RNA Isolation and Microarray Hybridization and Analysis*

Total RNA was isolated using Trizol (Invitrogen, Burlington, ON, Canada), following the manufacturer's protocol. Total RNA (20  $\mu\text{g}$ ) was converted to cDNA by incubation with 400 U of SuperScript II RT (Invitrogen) using a T7-oligo-d(T)<sub>24</sub> primer [5'-GGCCAGTG-AATTGTAATACGACTCACTATAGGGAGGCGG-(dT)<sub>24</sub>-3'], 1 $\times$  first-strand buffer (50 mM Tris·HCl, pH 8.3, 75 mM KCl, 3 mM MgCl<sub>2</sub>, 10 mM DTT), and 0.5 mM dNTPs at 42°C for 1 h. Second-strand synthesis was performed using 40 U of DNA polymerase I, *Escherichia coli* DNA ligase, 2 U of RNase H (Invitrogen), 1 $\times$  reaction buffer [18.8 mM Tris·HCl, pH 8.3, 90.6 mM KCl, 4.6 mM MgCl<sub>2</sub>, 3.8 mM DTT, 0.15 mM NAD, 10 mM (NH<sub>4</sub>)<sub>2</sub>SO<sub>4</sub>], and 0.2 mM dNTPs at 16°C for 2 h. cDNAs were blunt-ended with 10 U of T4 polynucleotide kinase (Invitrogen) incubated 5 min at 16°C. cDNA was then extracted with phenol-chloroform using phase lock gels (Brinkman, Mississauga, ON, Canada), ethanol precipitated, and resuspended in 10  $\mu\text{l}$  of diethyl pyrocarbonate-treated H<sub>2</sub>O. cDNA was *in vitro* transcribed using a T7 BioArray High Yield RNA Transcript Labeling Kit (Enzo Diagnostics, Farmingdale, NY) to produce biotinylated cRNA. The mixture (20- $\mu\text{l}$  final volume) was incubated at 37°C for 5 h, with gentle mixing every 30 min. Labeled cRNA was purified with an RNeasy Mini Kit (Qiagen, Valencia, CA) according to the manufacturer's protocol. Purified cRNA was then fragmented to 30- to 200-mer cRNA, using a fragmentation buffer (100 mM potassium acetate-30 mM magnesium acetate-40 mM Tris-acetate, pH 8.1), for 20 min at 94°C. The quality of total RNA, cDNA synthesis, cRNA amplification, and cRNA fragmentation was monitored by microcapillary electrophoresis (Bioanalyzer 2100; Agilent Technologies, Palo Alto, CA).

cRNA probes were hybridized to the MG-U74 v2 Genechip Set (Affymetrix, Santa Clara, CA). Fragmented cRNA (15  $\mu\text{g}$ ) was incubated with 1 $\times$  hybridization buffer (0.1 mg/ml herring sperm DNA, 0.5 mg/ml acetylated BSA, 5 nM control oligonucleotide B2) and 1 $\times$  eukaryotic hybridization control solution (1.5 pM *BioB*, 5 pM *BioD*, 25 pM *BioD*, and 100 pM *cre*) for 16 h at 45°C with constant rotation (60 rpm). The cRNA probe from the control group was hybridized on two microarrays (duplicate), while the cRNA probe corresponding to each time point was hybridized on separate microarrays. Microarrays were then processed using an Affymetrix Genechip Fluidic Station 400 (protocol EukGE-WS2Av4). Staining was performed with streptavidin-conjugated phycoerythrin (SAPE) followed by amplification with a biotinylated anti-streptavidin antibody and by a second round of SAPE solution. Genechips were scanned with the use of Genechip Scanner 3000 (Affymetrix). Signal intensities for  $\beta$ -actin and GAPDH genes were used as internal quality controls. The ratio of fluorescent intensities for 5' and 3' of these housekeeping genes was  $<2$ . Scanned images were analyzed and normalized (target intensity equal to 500) with Microarray Suite (MAS) 5.0 (Affymetrix).

Differentially expressed genes were selected using a variable-limit fold change (LFC) (44) decreasing with gene expression value [LFC =  $a + (b/x)$ , where  $x$  is the minimum intensity of gene expression]. The curve was estimated based on a ratio distribution calculated from replicated chips. The resulting cut-off point, LFC =  $1.9 + (\frac{60.0}{x})$ , produces an approximately constant rate of false positive-modulated genes of 0.1%. Genes over this criterion must also be called present at least in 2 points of the experiment using the MAS5.0 program. Affymetrix MAS5.0-normalized signal intensities were submitted to the Gene Expression Omnibus (GEO; <http://www.ncbi.nlm.nih.gov/geo/>) and are available under the following series ID: GSE6219.

### Clustering Analysis

The differentially expressed genes were clustered using GeneCluster2 software based on a self-organizing maps algorithm. Genes showing a maximum-to-minimum ratio >1.9-fold in their gene expression levels and >300 in their expression intensities were selected. Selected genes were then normalized to obtain a mean value of zero and a standard deviation of one. Finally, the normalized data were clustered. The expression patterns of certain PTPs and MKPs, as well as selected genes belonging to the IGF-I pathway, were validated by Q-RT-PCR. The L2L software was used to classify genes from each cluster into biological processes (45). When genes could not be classified by this software, EASE software (29) was used to identify the biological process associated with the gene. With the use of L2L, the fold enrichment of specific subclasses of general functions was also calculated along with the corresponding *P* value derived from a binomial distribution (when applicable). Genes were classified in more than one major biological process, since several proteins can demonstrate many different physiological activities in cell metabolism, which is more representative of the gene function.

### Q-RT-PCR

cDNA corresponding to 20 ng of total RNA coming from samples of a duplicated *in vivo* protocol was used to perform fluorescent-based real-time PCR quantification using the Light Cycler Real-Time PCR apparatus (Roche Inc, Nutley, NJ). Reagents were obtained from the same company and were used as described by the manufacturer. The conditions for PCR reactions were as follows: denaturation at 95°C for 10 s, annealing at 56–66°C for 5 s, and elongation at 72°C for 7–13 s. The reaction was then heated for 3 s at 2°C lower than the melting temperature of the DNA fragment. Reading of the fluorescence signal was taken at the end of the heating to avoid nonspecific signal. A melting curve was performed to assess nonspecific signal. Oligoprimers that allow the amplification of ~200 bp were designed by GeneTools software (Biotools, Edmonton, Alberta, Canada), and their specificity was verified by basic local alignment search tool in the GenBank database. Data calculation and normalization were performed using the second-derivative and double-correction method, as described previously (36a), and with use of the house-keeping gene hypoxanthine guanine phosphoribosyl transferase-1 (*Hprt1*). *Hprt1* gene is recognized to display stable expression levels from embryonic life through adulthood in various tissues (69). mRNA expression levels are expressed as number of copies per microgram of total RNA using a standard curve of *C<sub>p</sub>* vs. logarithm of the quantity, where *C<sub>p</sub>* is crossing point. The standard curve was established using known cDNA amounts of 10, 10<sup>2</sup>, 10<sup>3</sup>, 10<sup>4</sup>, 10<sup>5</sup>, and 10<sup>6</sup> copies of *Hprt1* and the Light Cycler 3.5 program provided by the manufacturer (Roche).

## RESULTS

### Microarray Analysis: Genomic Response of the Uterus to Estradiol

To study the time course of estradiol action on uterine physiology, we analyzed 1,141 genes regulated by E2 in the uterus. Among the selected genes, whose regulation is stimulated or repressed, seven individual profiles (A–G) are represented in Fig. 1 (for gene content of each cluster, see Supplemental Table S1; supplemental data are available at the online version of this article). For the clustering analysis, we used (1 × 4) node numbers for the E2-induced genes, while (1 × 3) node numbers were used for the downregulated genes. These node numbers are representative of the temporal change of the genes listed for a given clustering, as each of them gave independent clustering patterns. We can see that >64% (736) of the E2-modulated genes listed are stimulated. Moreover,

among the 736 genes upregulated by E2, four expression profiles clearly emerge: genes of *cluster A* (19%, 139 of 736) are induced within 3 h, genes of *cluster B* (37%, 274 of 736) within 6 h, and genes of *cluster C* (26%, 188 of 736) within 12 h, while genes of *cluster D* (18%, 135 of 736) are stimulated in the last phase of the 24-h period. The majority of genes stimulated by E2 are represented in *clusters B* and *C*. However, only three expression profiles are observed for the 405 genes that are downregulated by E2. Thus the genes of *cluster E* (25%, 101 of 405) are repressed within 6 h, while genes of *cluster F* (53%, 215 of 405) show a repression plateau between 6 and 12 h, and genes of *cluster G* (22%, 89 out of 405) are gradually repressed within 24 h. The majority of E2-downregulated genes are thus inhibited between 6 and 12 h (*cluster F*).

Following their expression pattern profile, genes from each cluster (*clusters A–G*) were then categorized into 10 different biological processes using the L2L and EASE softwares. The genes not assigned to a known function were classified as unknown biological process. For a given profile, the gene proportion of each function has been calculated and is illustrated in Fig. 2. According to the data presented in Fig. 2, it can be seen that, at specific times, E2 affects similarly genes having associated functions.

Indeed, among the stimulated genes (*clusters A, B, C, and D*), those involved in signal transduction and transcription represent the majority in *cluster A*, the latter group also being dominant in *cluster B* with genes associated with protein metabolism. The major gene functions found in *cluster C* are associated with protein metabolism and transport, while in *cluster D*, cell adhesion, development, and energy metabolism represent the major biological processes.

Among the downregulated genes represented (*clusters E, F, and G*), energy metabolism is the main biological process downregulated in *cluster E*, while in *cluster F*, there is a slight decrease of expression of genes implicated in signal transduction, transcription, and protein metabolism compared with *cluster E*. In *cluster G*, genes related to defense and inflammation appear in preponderance.

*Specific early modulated genes: 0–6 h (clusters A, B, and E).* As shown in Fig. 3, the genes associated with signal transduction were predominantly observed in *cluster A*, especially those belonging to the protein kinase cascade, the MAPKK cascade, and mRNA catabolism, which demonstrated a fold enrichment of 3.6, 5.7, and 11.1, respectively. Several transcription regulators like *Fos*, *Junb*, and *Egr1* are well recognized as E2-responsive genes (12, 14, 36). The genes involved in translation, ribosome biogenesis, and amino acid activation are particularly enriched in *cluster B* in a range covering 6- to 10.8-fold. The downregulated genes included in *cluster E* are involved in fatty acid and aldehyde metabolisms (34).

*Specific late-modulated genes: 6–24 h (clusters C, D, F, and G).* As also demonstrated in Fig. 3, the transport molecules and genes involved in protein metabolism represent the major groups in *cluster C*, particularly the genes associated with intracellular transport (3.6-fold), cellular localization (3.5-fold), protein targeting (5.5-fold), and actomyosin structure organization and biogenesis (29.9-fold). In *cluster D*, there is an overexpression of genes involved in cell adhesion, development, and energy metabolism. Particularly, genes implicated in epidermis and ectoderm development, tissue development

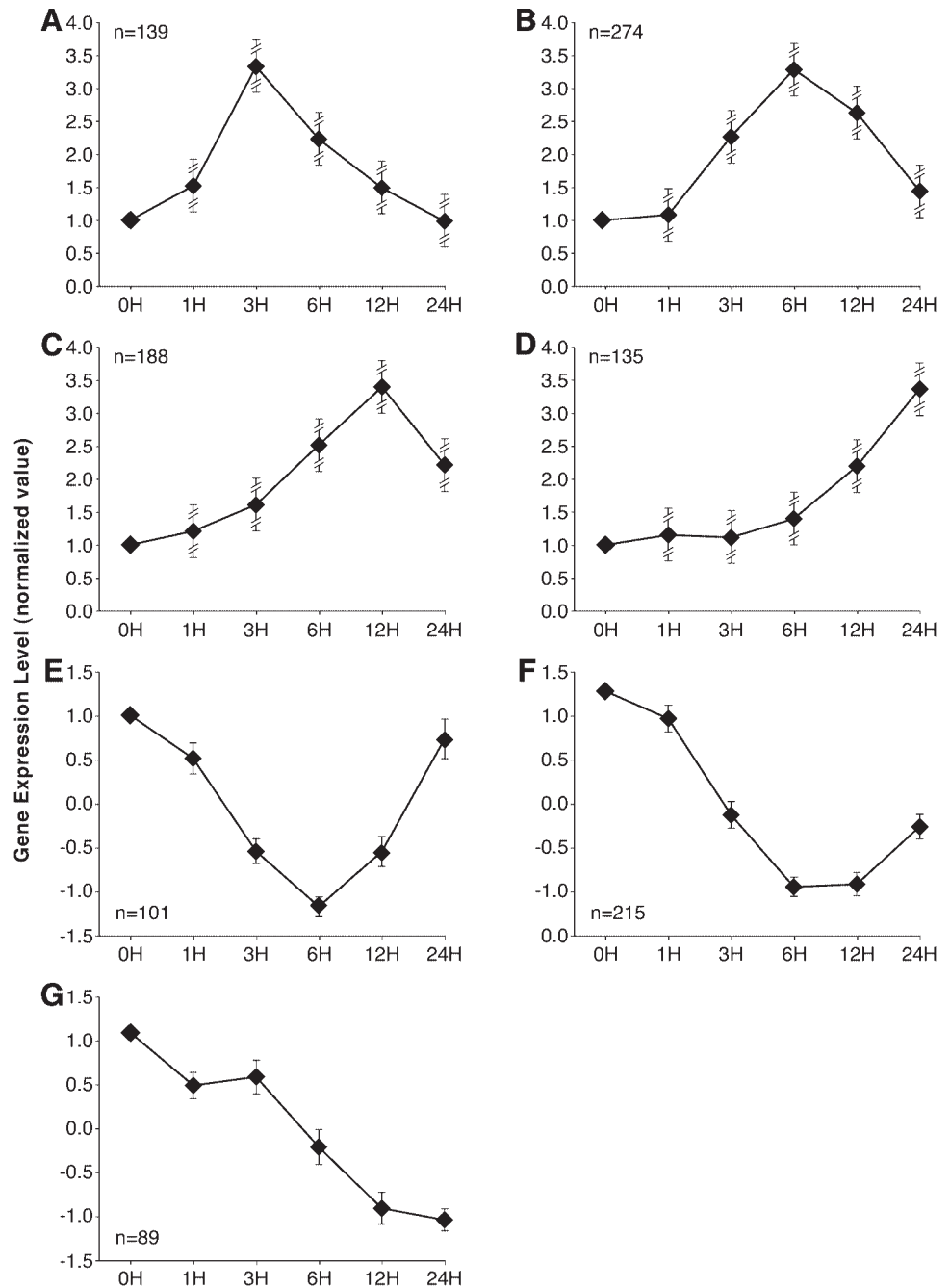


Fig. 1. Clustering of gene expression patterns. Among 1,141 genes that passed the variation filter, 736 upregulated genes and 405 downregulated genes were normalized to obtain a mean equal to 0 and an SD equal to 1 across time points, separately. After the normalization, with the use of a self-organizing map (GeneCluster2), they were grouped into 4 clusters (A–D) and 3 clusters (E–G) of activated and inhibited genes, respectively. Each cluster is represented by the centroid of normalized values on the y-axis and time points on the x-axis, where H is hour(s). The number of genes belonging to each cluster is displayed. These patterns indicate the representative temporal gene expression changes of the selected genes. Error bars indicate the maximal and minimal fold value for A–D and the SD of the average expression levels for E–G.

and keratinocyte differentiation, and carbohydrate and cholesterol metabolism (34) display an overabundance ranging from 7.1- to 41-fold. The processes related to cell growth and apoptosis are also slightly more represented in this cluster compared with clusters A, B, and C (see Supplemental Table S1), which is consistent with the modulation of several cell cycle components described by Tong and Pollard (65).

In cluster F, downregulated genes specifically involved in bone metabolism and cell differentiation are identified, with a fold enrichment of 14.8 and 7.1, respectively. Cluster G displays a significantly lower expression of genes related to immunity and RNA processing, particularly genes associated with antigen presentation and processing (human leukocyte antigen genes), which show a fold enrichment of 15.5.

Taken together, these observations point toward evidence of a rapid induction of transcriptional regulators and signaling component genes, followed by a late induction of cytoarchitectural genes, which have been well demonstrated in previous studies (27, 39, 70). Additionally, this study shows a significant time-dependent gradual diminution of specific genes involved in immunity and inflammation.

#### Estradiol Modulates the IGF-I Pathway

To confirm the temporal changes of gene expression levels of certain genes involved in the IGF-I pathway, Q-RT-PCR was performed (Fig. 4). Briefly, six IGF-related genes, three Ras/Raf/MAPK pathway-related genes, three PIK3 pathway-related genes,

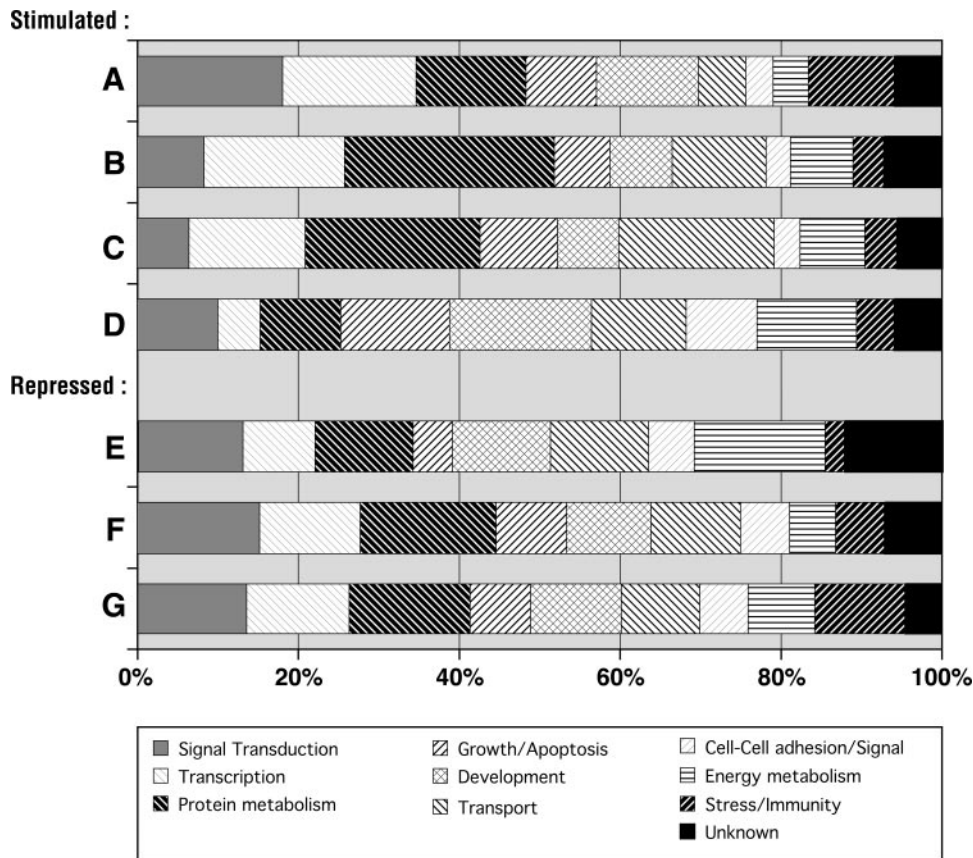


Fig. 2. Functional classification of clustered genes. Different functions of the clustered genes were grouped into 10 categories using L2L and EASE softwares, and the percent representation of each function is indicated. Each corresponding cluster, as described in Fig. 1.

and five tyrosine and MAP kinase phosphatase genes were analyzed. All genes tested displayed an 82% correlation rate between microarrays and Q-RT-PCR.

**IGF-related genes.** In the present study, the IGF-I gene is induced within 12 h (Fig. 4A). Interestingly, its receptor, IGF-IR, is downregulated within 6 h. The expression of IGFBP2 and -6 are increased and decreased, respectively, within 12 h. Moreover, the IGFBP3 gene is inhibited within 12 h, while the IGFBP5 gene is stimulated within 24 h. Our results are therefore consistent with these previous findings (27, 39, 70), although IGF-IR and IGFBP6 were not identified as genes regulated by E2 in a similar study performed by Hewitt et al. (27).

**Ras/Raf/MAPK pathway.** Expression of the Cdc25c gene is strongly increased between 6 and 24 h (Fig. 4B). Furthermore, most Ras genes (Ran, Ras12-9) are also induced within 3 h (see Supplemental Table S1). Then, MAPK1 (ERK2) expression shows a slight repression plateau between 6 and 18 h. The expression of the c-Myc gene is increased within 3 h, and expressed sequence tags (ESTs) similar to putative c-Myc-responsive genes (*Homo sapiens*) are induced within 18 h. In fact, c-Myc is an immediate early gene known to be activated after stimulation of the MAPK signal transduction pathway (11, 24). Following E2 treatment, the structural ornithine decarboxylase gene (ODC) is also upregulated within 6 h, its protein activity being well known to be induced after exposure to E2 in a tissue such as the uterus (72). Indeed, the ERK1/ERK2 activation has been shown to be essential for ODC induction, which is associated with cell proliferation (21, 57).

**PI3K pathway.** From Fig. 4B, it can be seen that the expression of GAB1 and PIK3R2 genes is decreased within

6 h, while the SH3-domain GRB2-like B1 gene (SH3GLB1), which codes for an endophilin cell death promoter, is first slightly upregulated within 3 h and then inhibited between 6 and 12 h (data not shown). The BCL2-like 11 (apoptosis facilitator) gene is also downregulated within 12 h. The IGF-I activation of the PIK3 pathway is known to promote an anti-apoptotic effect (68).

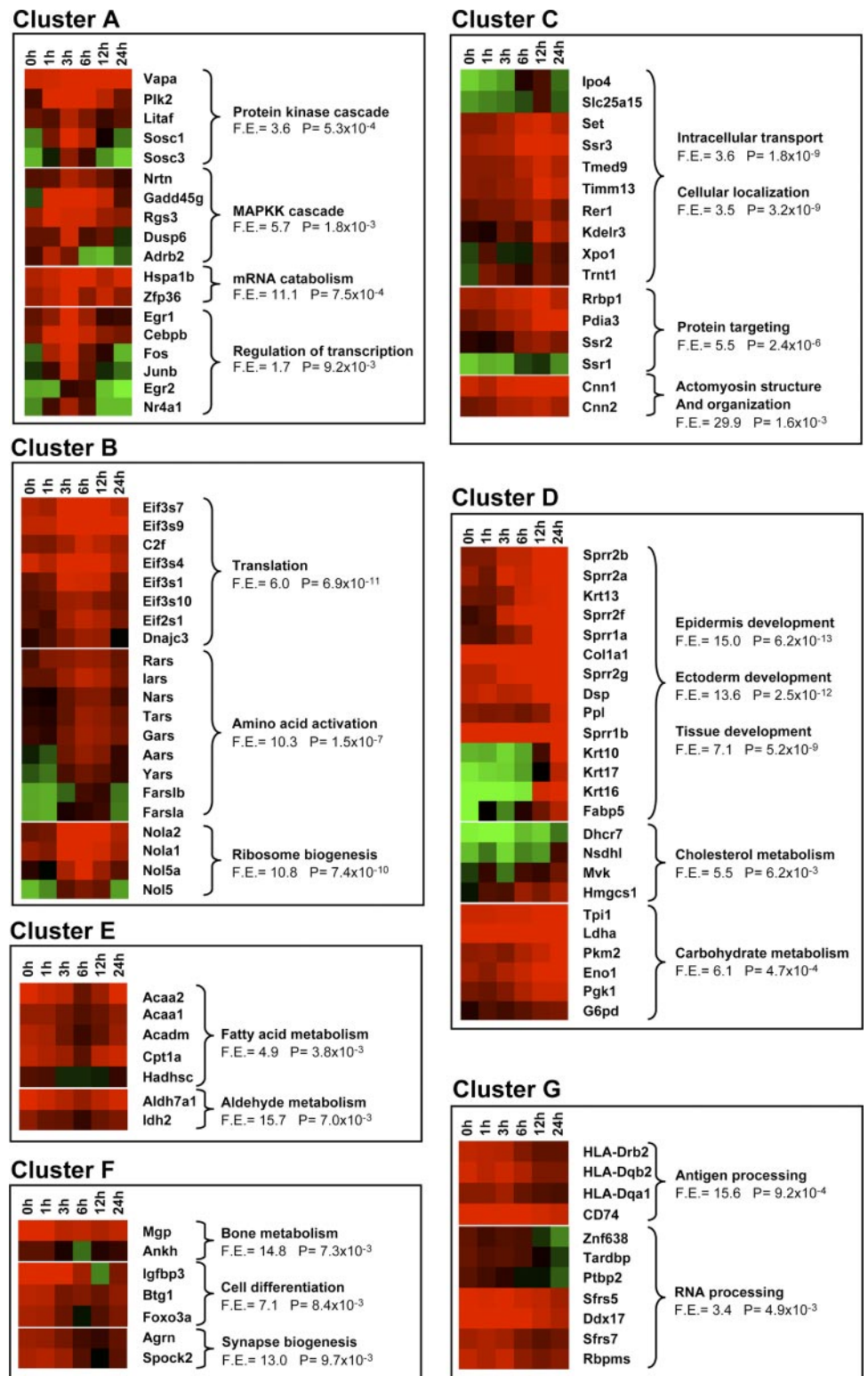
**Tyrosine and MAP kinase phosphatases.** As shown in Fig. 4C, the PTP genes PTP1B and PTP4A are early induced by E2 within 3 h. Similarly, MAP kinase phosphatase genes MKP1 and MKP3 are upregulated within 3 h. Then the STEP gene, whose product is known to deactivate the phosphotyrosine activity of ERK1/2 (associated with mitogenesis) (54), is induced within 6 h. The MKP1 gene product is also known to deactivate ERK (MAPK) (60), and the MKP3 gene product dephosphorylates the activated ERK2 (MAPK1) (43). Another gene belonging to this class is PTP1B, whose protein inhibits the activity of the full-length IGF-IR in mammals, while the product of PTP4A has been reported to stimulate cell growth and could be involved in tumorigenesis (10).

Taken together, these observations suggest that, as presented in Fig. 5, the PTPs and MKPs could be potentially closely involved in the extent and duration of the E2 uterotrophic effect in mice by targeting the IGF-I pathway.

## DISCUSSION

In the present study, ovariectomized mice were exposed to a physiological dose of E2 up to 24 h. Our global data demonstrate that a physiological dose of E2 (2.5  $\mu$ g/kg) can

Fig. 3. Relevant list (selected subgroups) of up- and downregulated genes in each cluster. The gene names and Affymetrix probe set numbers in each cluster (lettered A–G) are indicated. Changes in expression levels are also indicated by color based on normalized values (green and red for low and high values, respectively) with the time points (in h) indicated above. Major subclasses of gene functions with their corresponding fold enrichment (FE) and *P* value (*P*) are also displayed for each cluster.



trigger uterotrophic effects similar to those observed when using a supraphysiological dose (5–50  $\mu\text{g}/\text{kg}$ ) (27, 39, 70). However, as discussed in greater detail below, this physiological dose seems to activate groups of genes having similar functions in a more homogenous fashion than observed in other studies (e.g., major IGFEBPs and keratiniza-

tion-associated molecules are detected and regulated in an expected manner, i.e., genes involved in cell cycle stimulation are upregulated and genes involved in cell cycle arrest are downregulated).

The major cell cycle- and intracellular trafficking-related genes involving, notably, the protein kinase and MAPKK

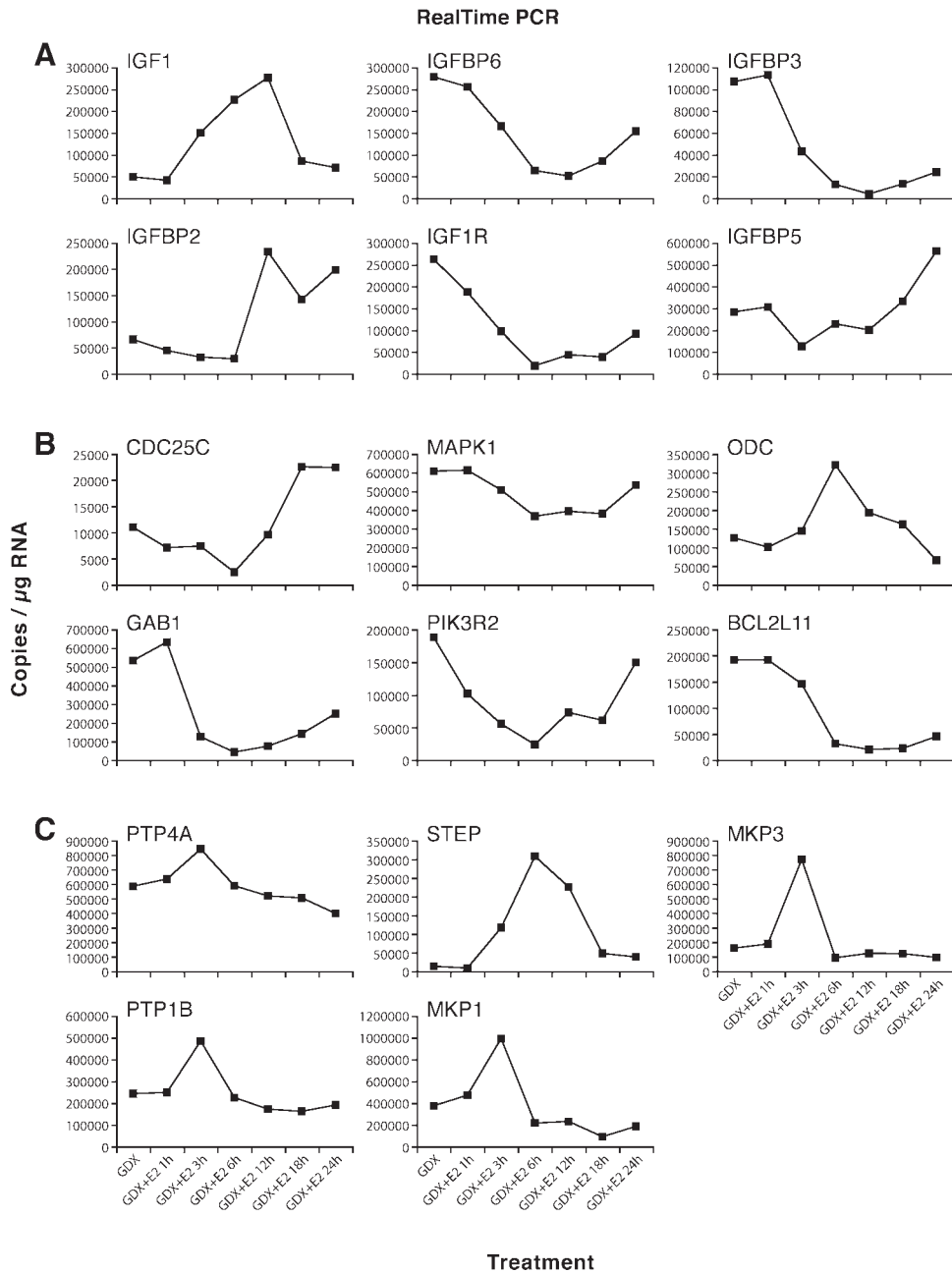


Fig. 4. Temporal changes of gene expression levels performed by quantitative real-time PCR (Q-RT-PCR). Evidence for a transcriptional regulatory network during the uterotrophic response of insulin-like growth factor (IGF)-related genes (A), genes involved in MAPK and phosphatidylinositol 3-kinase (PIK3) pathways (B), and tyrosine and MAP kinase phosphatase-related genes (C). The number of copies per  $\mu\text{g}$  RNA is indicated on the y-axis and the time points on the x-axis. IGFBP, IGF binding protein; IGF-IR, IGF-I receptor; ODC, ornithine decarboxylase; MKP, MAPK phosphatase; PTP, protein tyrosine phosphatase.

signaling cascades and heat shock protein (HSP) genes are upregulated early, i.e., within 0–6 h. Indeed, it has been shown that some HSPs would participate in cell proliferation by interacting with proteins needed for the proliferation process (50). Specifically, the oncogenes Fos and Junb are quickly upregulated (within 3 h), these genes being known to be rapidly induced by E2 (12, 36, 70). In addition, as previously reported for some of these genes (14, 39, 70), we observed that most signal transduction-related genes, transcription factors such as Egr1, Egr2, Cebpb and Nr4a1, and ribosomal protein genes are also stimulated during the first phase of the E2 effect (from 0 to 6 h). Taken together, these results are in line with previous observations confirming that, among E2-regulated genes in the mouse uterus, early induced transcription factors may play an important role in subsequent changes in gene

expression (70), further suggesting that, in response to E2, a transcriptional cascade may operate in the uterus (39). Cardenas et al. (9) recently reported that the administration of E2 to ovariectomized gilts increased uterine weight. It is well known that proestrous in rodents is characterized by proliferation of endometrial cells accompanied by a gradual increase of estrogen concentrations (62). Interestingly, in contrast to previous studies, we report here for the first time that the Gadd45g gene is markedly stimulated very early (31.3-fold). Indeed, this gene has not been reported in previous studies (27, 39, 70). This regulation can, however, be taken seriously, given the additional confirmation by Q-RT-PCR and the modulation of several other known E2-responsive genes present in this study. Although no estrogen response elements (EREs) are present in the proximal region of the promoter of the Gadd45g gene, the

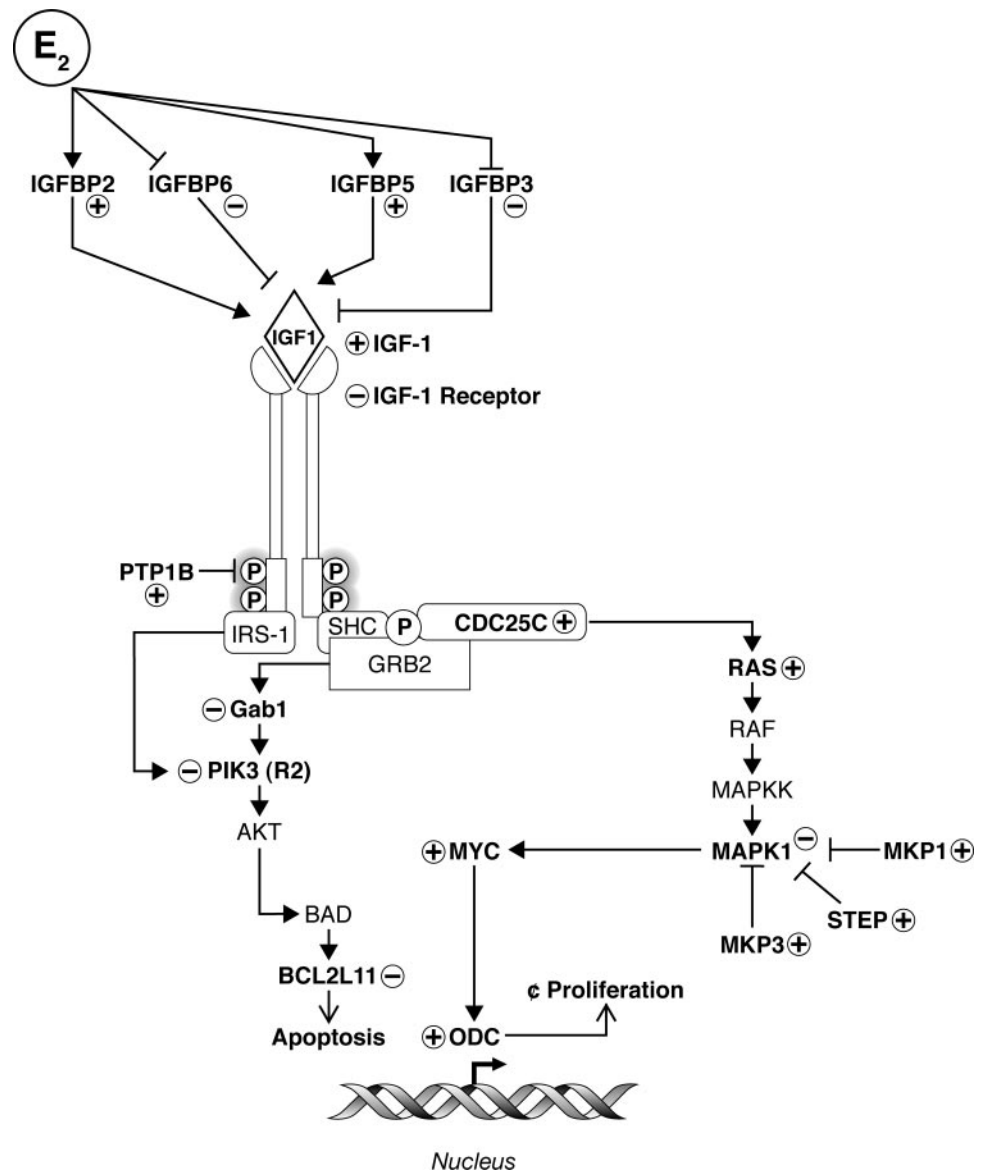


Fig. 5. Schematic representation of the transcriptional cascade triggered by 17 $\beta$ -estradiol (E<sub>2</sub>) following activation of the IGF-1 pathway. E<sub>2</sub> activates a transcriptional cascade resulting in an uterotrophic effect in mouse. Genes confirmed by Q-RT-PCR are highlighted in bold, and their E<sub>2</sub> modulation, stimulation or repression, is indicated in circles by + or - symbols, respectively.

presence of many SP1 sites could explain this regulation. Gadd45 proteins are involved in negative growth control, rendering this observation to be investigated more extensively. Interestingly, Gadd45g interacts with p21 and especially proliferative cell nuclear antigen (PCNA), which has been demonstrated to impede its effect on cell cycle arrest (2), as also observed for Gadd45 $\alpha$  and Gadd45 $\beta$  (66).

According to previous results (27, 39, 70), peptidase and protease genes reach their peak of expression at 12 h. It has been shown that peptidases, proteases, and their inhibitors could play an important role in balancing the uterine environment for appropriate sperm activity and the periodic remodeling of the uterine endometrium (62). Genes involved in intracellular transport and localization as well as protein targeting are also particularly predominant at 12 h. In agreement with the uterotrophic effect of E<sub>2</sub>, our data show a gradual upregulation (until 24 h) of most structural and cytoskeleton, extracellular matrix, and cell adhesion genes required for tissue development, which is also consistent with previous studies (27, 39, 70).

Interestingly, our data reveal a global modulation of many molecules associated with keratinization processes, mainly observed in *cluster D*, which is consistent with the cytoarchitectural structure evolution. In addition to the small proline-rich proteins (Sprr)-1A and -2A described previously by Hewitt et al. (27), we also report here the upregulation of Sprr1B, -2B, -2D, -2F, and -2G. Moreover, in addition to the keratin complex 1 gene-13 (Krt1-13) and -19 and Krt2-6a previously reported as E<sub>2</sub> regulated (27), the data presented here also display the upregulation of Krt1-10, -16, -17, and -18 and Krt2-18 and -7 (*cluster D*) (see Supplemental Table S1). Therefore, as these above-mentioned regulations appear in conjunction with other genes known to be E<sub>2</sub> responsive, it strengthens the reliability of data obtained and the efficacy of treatment.

Although the number of downregulated genes is more limited, we can point out the downregulation of inflammation genes occurring in the late phase (between 12 and 24 h). Besides, this downregulation, resulting in reduced levels of

autoimmune disease activity, has been reported to correlate with high levels of circulating estrogen during pregnancy (1). Previous findings have also demonstrated that E2 has opposing effects on bone marrow lymphoid and myeloid differentiation (49). In concordance with these results, our data show that most of the immune genes early induced code for myeloid precursor-differentiated molecules, while the late-downregulated genes code mainly for lymphoid precursor-differentiated molecules (see Supplemental Table S1). Therefore, E2 may serve in promoting the myeloid-differentiated molecules action as well as inhibiting the lymphoid-differentiated molecules action in the mouse uterus.

Estrogens are known to behave as proadipogenic factors, and IGF-I has been shown to stimulate both growth and differentiation of preadipocytes (17). In this study, the expression of both lipid transport- and metabolism-related genes is decreased and then later increased by E2, which has not been observed in other studies. Interestingly, it has been suggested, although not significantly, that E2 could potentially downregulate triglycerides in liver, although it significantly induces serum triglycerides, while serum high-density lipoproteins seem to be slightly reduced in ovariectomized rats (23, 35, 53).

To further support our observations, we have developed a scheme illustrating how IGF-I pathway components interact and affect one another (Fig. 5). Consistent with the global expression profile revealed by our data, it has been suggested that IGF-I is a mediator of the E2 uterotrophic effect in the rat uterus (30, 42). The IGF-BPs bind specifically to IGF-I with high affinity (18). As observed previously (40), the expression of IGF-BP genes that inhibit the IGF-I effect (IGFBP3 and -6) appears to be repressed by E2, this inhibitory effect of IGFBP3 being well demonstrated in fibroblast cells (18), whereas the expression of IGF-BP genes that potentiate the IGF-I effect (IGFBP2 and -5) is stimulated by E2, as previously reported in vascular endothelial cells (4).

In fact, these gene products are known to facilitate interaction with the receptor. Interestingly, IGFBP2 and -3 have been detected respectively in the luminal epithelium and in the stromal cells of the endometrium, while IGFBP5 and -6 are expressed in the myometrium (22). IGF-I binds to its receptor and induces a transphosphorylation that activates multiple signals that promote cellular proliferation. Indeed, it has been shown that a sustained increase in the tyrosine phosphorylation of IGF-IR and IRS-1 can be caused by E2 in the endometrial epithelial cells of ovariectomized mice (55).

E2 can then induce an IGF-I-activated signal transduction of the PIK3 and Ras/Raf/MAPK pathways. The E2 activation of the PIK3 protein thereafter induces the phosphorylation of AKT in endometrial cells (25) and the inactivation of the proapoptotic protein BAD, a member of the Bcl2 family that regulates the apoptotic response. E2 also inhibits SH3GLB1, an endophilin known to interact with the proapoptotic protein BAX and to promote cell death in mouse hematopoietic cells following interleukin-3 withdrawal (13), these genes being well known to contribute to apoptosis protection (52). Activation of the MAPK pathway has been shown to induce a transcriptional response associated with mitogenesis (38) and cell motility (6, 15, 64). As a consequence, genes that play important roles in cell proliferation induction, like c-Myc and ODC in this study, are upregulated following E2 stimulation of the MAPK signal transduction pathway. It has also been shown

that the overexpression of ERK2 (MAPK1) activates Myc (11). Consistent with these results, Inoue et al. (31) recently suggested that endometrial IGF-I stimulates proliferation of mouse endometrial stromal cells, and that the MAPK pathway is involved in DNA replication of endometrial stromal cells. However, our results also show a slight E2 inhibition of the expression of the ERK2 (MAPK1) gene involved in the MAPK pathway and whose protein is phosphorylated after E2 exposure (Fig. 5). This could be explained by the activation of STEP, MKP3, and MKP1, whose gene products have been reported to inhibit MAPK1 (74). Moreover, it has to be stated that Myc can also be quickly transcriptionally activated by the direct action of E2, through the EREs present in its promoter (19).

In addition, IGF-IR overexpression and/or its constitutive activation have been associated with malignant transformation and have been linked to the metastatic properties of tumor cells. Particularly, endometrial tumors are more likely to overexpress IGF-IR (48). In the present data, IGF-IR is downregulated by E2, consistent with a cancer-free state. This could be explained by the activation of PTP1B, whose gene product has been shown to inhibit the tyrosine activity of full-length IGF-IR in mammalian cells (7). Analogous to what is seen in cardiac cells, where E2 increases MKP1 expression (61), we show that, in the uterus, E2 promotes the early induction of protein tyrosine and MKP genes such as PTP1B, MKP1, MKP3, and STEP, whose proteins target certain activated components of the IGF-I pathway, suggesting that these phosphatases may act as a negative control on IGF-I signaling in the mouse uterus. In the present study, E2 also downregulates some IGF-I pathway key components such as IGF-IR and MAPK1 (ERK2). However, the IGF-IR signaling pathways exhibit redundancy because of considerable cross talk among them (47). There is also evidence of an E2 regulation of IGF-I via androgen receptor (AR) production (51, 71) and of cross talk in IGF-IR and estrogen receptor signaling (26, 42, 68), thus illustrating the complexity of this process.

Our data support and confirm previous findings that E2 activates a transcriptional cascade resulting in an uterotrophic effect in the mouse. To control this process, E2 induces concomitantly genomic (gene modulation) and nongenomic (phosphorylation/dephosphorylation) mechanisms, although the changes observed in this study are all genomic, since they seem to result from altered gene expression. Although gene transcription changes represent a major cause of altered signaling pathways, we cannot exclude other nongenomic mechanisms, especially those involved in transduction signaling, that could be important mechanisms triggering protein level variations. A comprehensive knowledge of these mechanisms would be extremely useful for understanding the evolution and progression of uterine cancers as well as gynecological diseases and infertility. The role of the IGF-I pathway appears to be pivotal in this process, and therefore more work is definitely needed to further progress in this field.

#### GRANTS

This work was supported by Genome Canada and Genome Québec for the "ATLAS of genomic profiles of steroid action" project. M. Ivanga is a recipient of a Canadian Institutes of Health Research (CIHR) studentship as part of a training program in genomics ("Génomique fonctionnelle des maladies endocriniennes") and of a studentship of the Gabonese government. F. Durocher is a recipient of a Research Career Award in Health Sciences by the CIHR/Research and Development Health Research Foundation.

## REFERENCES

1. Adamski J, Ma Z, Nozell S, Benveniste EN. 17beta-Estradiol inhibits class II major histocompatibility complex (MHC) expression: influence on histone modifications and cbp recruitment to the class II MHC promoter. *Mol Endocrinol* 18: 1963–1974, 2004.
2. Azam N, Azam N, Vairapandi M, Zhang W, Hoffman B, Liebermann DA. Interaction of CR6 (GADD45gamma) with proliferating cell nuclear antigen impedes negative growth control. *J Biol Chem* 276: 2766–2774, 2001.
3. Baker J, Hardy MP, Zhou J, Bondy C, Lupu F, Bellve AR, Efstratiadis A. Effects of an Igf1 gene null mutation on mouse reproduction. *Mol Endocrinol* 10: 903–918, 1996.
4. Bar RS, Booth BA, Boes M, Dake BL. Insulin-like growth factor-binding proteins from vascular endothelial cells: purification, characterization, and intrinsic biological activities. *Endocrinology* 125: 1910–1920, 1989.
5. Bhalla US, Ram PT, Iyengar R. MAP kinase phosphatase as a locus of flexibility in a mitogen-activated protein kinase network. *Science* 297: 1018–1023, 2002.
6. Bonacchi A, Romagnani P, Romanelli RG, Efsen E, Annunziato F, Lasagni L, Francalanci M, Serio M, Laffi G, Pinzani M, Gentilini P, Marra F. Signal transduction by the chemokine receptor CXCR3: activation of Ras/ERK, Src, and phosphatidylinositol 3-kinase/Akt controls cell migration and proliferation in human vascular pericytes. *Biol Chem* 276: 9945–9954, 2001.
7. Buckley DA, Loughran G, Murphy G, Fennelly C, O'Connor R. Identification of an IGF-1R kinase regulatory phosphatase using the fission yeast *Schizosaccharomyces pombe* and a GFP tagged IGF-1R in mammalian cells. *Mol Pathol* 55: 46–54, 2001.
8. Buttram VC Jr, Reiter RC. Uterine leiomyomata: etiology, symptomatology, and management. *Fertil Steril* 36: 433–445, 1981.
9. Cárdenas H, Pope WF. Attenuation of estrogenic effects by dihydrotestosterone in pig uterus is associated with downregulation of the estrogen receptors. *Biol Reprod* 70: 297–302, 2004.
10. Cates CA, Michael RL, Stayrook KR, Harvey KA, Burke YD, Randall SK, Crowell PL, Crowell DN. Prenylation of oncogenic human PTP(CAAX) protein tyrosine phosphatases. *Cancer Lett* 110: 49–55, 1996.
11. Chuang CF, Ng SY. Functional divergence of the MAP kinase pathway ERK1 and ERK2 activate specific transcription factors. *FEBS Lett* 346: 229–234, 1994.
12. Cicatiello L, Sica V, Bresciani F, Weisz A. Identification of a specific pattern of “immediate-early” gene activation induced by estrogen during mitogenic stimulation of rat uterine cells. *Receptor* 3: 17–30, 1993.
13. Cuddeback SM, Yamaguchi H, Komatsu K, Miyashita T, Yamada M, Wu C, Singh S, Wang HG. Molecular cloning and characterization of Bif-1: a novel Src homology 3 domain-containing protein that associates with Bax. *J Biol Chem* 276: 20559–20565, 2001.
14. de Jager T, Pelzer T, Muller-Botz S, Imam A, Muck J, Neyses L. Rapid gene activation via the ERK1/2 pathway and serum response elements. *J Biol Chem* 276: 27873–27880, 2001.
15. Delehede M, Sergeant N, Lyon M, Rudland PS, Fernig DG. Hepatocyte growth factor/scatter factor stimulates migration of rat mammary fibroblasts through both mitogen-activated protein kinase and phosphatidylinositol 3-kinase/Akt pathways. *Eur J Biochem* 268: 4423–4429, 2001.
16. Deligdisch L, Holinka CF. Endometrial carcinoma: two diseases? *Cancer Detect Prev* 10: 237–246, 1987.
17. Dieudonne MN, Pecquery R, Leneuve MC, Giudicelli Y. Opposite effects of androgens and estrogens on adipogenesis in rat preadipocytes: evidence for sex- and site-related specificities and possible involvement of insulin-like growth factor 1 receptor and peroxisome proliferator-activated receptor g2. *Endocrinology* 141: 649–656, 2000.
18. Duan C, Xu Q. Roles of insulin-like growth factor (IGF) binding proteins in regulating IGF actions. *Gen Comp Endocrinol* 142: 44–52, 2005.
19. Dubik D, Shiu RP. Mechanism of estrogen activation of c-myc oncogene expression. *Oncogene* 7: 1587–1594, 1992.
20. Farquhar CM. Extracts from the “clinical evidence.” *Endometriosis BMJ* 320: 1449–1452, 2000.
21. Flamigni F, Facchini A, Giordano E, Tantini B, Stefanelli C. Signaling pathways leading to the induction of ornithine decarboxylase: opposite effects of p44/42 mitogen-activated protein kinase (MAPK) and p38 MAPK inhibitors. *Biochem Pharmacol* 61: 25–32, 2001.
22. Girvigian MR, Nakatani A, Ling N, Shimasaki S, Erickson GF. Insulin-like growth factor binding proteins show distinct patterns of expression in the rat uterus. *Biol Reprod* 51: 296–302, 1994.
23. Goss PE, Qi S, Cheung AM, Hu H, Mendes M, Pritzker KPH. The selective estrogen receptor modulator SCH 57068 prevents bone loss, reduces serum cholesterol and blocks estrogen-induced uterine hypertrophy in ovariectomized rats. *J Steroid Biochem* 92: 79–87, 2004.
24. Gupta S, Davis RJ. MAP kinase binds to the NH<sub>2</sub>-terminal activation domain of c-Myc. *FEBS Lett* 353: 281–285, 1994.
25. Guzeloglu-Kayisli O, Kayisli UA, Luceli G, Arici A. In vivo and in vitro regulation of AKT activation in human endometrial cells is estrogen dependent. *Biol Reprod* 71: 714–721, 2004.
26. Hewitt SC, Collins J, Grissom S, Deroo B, Korach KS. Global uterine genomics in vivo: microarray evaluation of the estrogen receptor alpha-growth factor cross-talk mechanism. *Mol Endocrinol* 19: 657–668, 2005.
27. Hewitt SC, Deroo BJ, Hansen K, Collins J, Grissom S, Afshari CA, Korach KS. Estrogen receptor-dependent genomic responses in the uterus mirror the biphasic physiological response to estrogen. *Mol Endocrinol* 17: 2070–2083, 2003.
28. Hickey M, Fraser I. Human uterine vascular structures in normal and diseased states. *Microsc Res Tech* 60: 377–389, 2003.
29. Hosack DA, Dennis G Jr, Sherman BT, Lane HC, Lempicki RA. Identifying biological themes within lists of genes with EASE. *Genome Biol* 4: R70, 2003.
30. Huynh H. Suppression of uterine insulin-like growth factor binding protein 5 by estrogen is mediated in part by insulin-like growth factor I. *Int J Oncol* 12: 427–432, 1998.
31. Inoue A, Takeuchi S, Takahashi S. Insulin-like growth factor-I stimulated DNA replication in mouse endometrial stromal cells. *J Reprod Dev* 51: 305–313, 2005.
32. Kao LC, Germeyer A, Tulac S, Lobo S, Yang JP, Taylor RN, Osteen K, Lessey BA, Giudice LC. Expression profiling of endometrium from women with endometriosis reveals candidate genes for disease-based implantation failure and infertility. *Endocrinology* 144: 2870–2881, 2003.
33. Kawakami A, Nakashima T, Tsuboi M, Urayama S, Matsuoka N, Ida H, Kawabe Y, Sakai H, Migita K, Aoyagi T, Nakashima M, Maeda K, Eguchi K. Insulin-like growth factor I stimulates proliferation and Fas-mediated apoptosis of human osteoblasts. *Biochem Biophys Res Commun* 247: 46–51, 1998.
34. Liang CP, Tall AR. Transcriptional profiling reveals global defects in energy metabolism, lipoprotein, and bile acid synthesis and transport with reversal by leptin treatment in ob/ob mouse liver. *J Biol Chem* 276: 49066–49076, 2001.
35. Liu ML, Xu X, Rang WQ, Li YJ, Song HP. Influence of ovariectomy and 17beta-estradiol treatment on insulin sensitivity, lipid metabolism and post-ischemic cardiac function. *Int J Cardiol* 97: 485–493, 2004.
36. Loose-Mitchell DS, Chiappetta C, Stancel GM. Estrogen regulation of c-fos messenger ribonucleic acid. *Mol Endocrinol* 2: 946–951, 1988.
- 36a. Luu-The V, Paquet N, Calvo E, Cumps J. Improved Real-Time RT-PCR method for high-throughput measurements using second derivative calculation and double correction. *Biotechniques* 8: 287–293, 2005.
37. Matias-Guiu X, Catusas L, Bussaglia E, Lagarda H, Garcia A, Pons C, Munoz J, Arguelles R, Machin P, Prat J. Molecular pathology of endometrial hyperplasia and carcinoma. *Hum Pathol* 32: 569–577, 2001.
38. Mii S, Khalil RA, Morgan KG, Ware JA, Kent KC. Mitogen-activated protein kinase and proliferation of human vascular smooth muscle cells. *Am J Physiol Heart Circ Physiol* 270: H142–H150, 1996.
39. Moggs JG, Tinwell H, Spurway T, Chang HS, Pate I, Lim FL, Moore DJ, Soames A, Stuckey R, Currie R, Zhu T, Kimber I, Ashby J, Orphanides G. Phenotypic anchoring of gene expression changes during estrogen-induced uterine growth. *Environ Health Perspect* 112: 1589–1606, 2004.
40. Molnar P, Murphy LJ. Effects of oestrogen on rat uterine expression of insulin-like growth factor-binding proteins. *J Mol Endocrinol* 13: 59–67, 1994.
41. Moreno-Bueno G, Sánchez-Estévez C, Cassia R, Rodríguez-Perales S, Diaz-Uriarte R, Dominguez O, Hardisson D, Andujar M, Prat J, Matias-Guiu X, Cigudosa JC, Palacios J. Differential gene expression profile in endometrioid and nonendometrioid carcinoma: STK15 is frequently overexpressed and amplified in nonendometrioid carcinomas. *Cancer Res* 63: 5697–5702, 2004.
42. Moyano P, Rotwein P. Mini-review: estrogen action in the uterus and insulin-like growth factor-I. *Growth Horm IGF Res* 14: 431–435, 2004.

43. **Muda M, Boschert U, Dickinson R, Martinou JC, Martinou I, Camps M, Schlegel W, Arkinstall S.** MKP-3, a novel cytosolic protein-tyrosine phosphatase that exemplifies a new class of mitogen-activated protein kinase phosphatase. *J Biol Chem* 271: 4319–4326, 1996.
44. **Mutch DM, Berger A, Mansourian R, Rytz A, Roberts MA.** The limit fold change model: a practical approach for selecting differentially expressed genes from microarray data. *BMC Bioinformatics* 3: 17, 2002.
45. **Newman JC, Weiner AM.** L2L: a simple tool for discovering the hidden significance in microarray expression data. *Genome Biol* 6: R81, 2005.
46. **Niklaus AL, Aberdeen GW, Babischkin JS, Pepe GJ, Albrecht ED.** Effect of estrogen on vascular endothelial growth/permeability factor expression by glandular epithelial and stromal cells in the baboon endometrium. *Biol Reprod* 68: 1997–2004, 2003.
47. **O'Connor R.** Regulation of IGF-1 receptor signaling in tumor cells. *Horm Metab Res* 35: 771–777, 2003.
48. **Ouban A, Muraca P, Yeatman T, Coppola D.** Expression and distribution of insulin-like growth factor-1 receptor in human carcinomas. *Hum Pathol* 34: 803–808, 2003.
49. **Paharkova-Vatchkova V, Maldonado R, Kovats S.** Estrogen preferentially promotes the differentiation of CD11c+ CD11b(intermediate) dendritic cells from bone marrow precursors. *J Immunol* 172: 1426–1436, 2004.
50. **Parcellier A, Gurbuxani S, Schmitt E, Solary E, Garrido C.** Heat shock proteins, cellular chaperones that modulate mitochondrial cell death pathways. *Biochem Biophys Res Commun* 304: 505–512, 2003.
51. **Pelletier G, Luu-The V, Li S, Labrie F.** Localization and estrogenic regulation of androgen receptor mRNA expression in the mouse uterus and vagina. *J Endocrinol* 180: 77–85, 2004.
52. **Perillo B, Sasso A, Abbondanza C, Palumbo G.** 17beta-Estradiol inhibits apoptosis in MCF-7 cells, inducing bcl-2 expression via two estrogen-responsive elements present in the coding sequence. *Mol Cell Biol* 20: 2890–2901, 2000.
53. **Picard F, Deshaies Y, Lalonde J, Samson P, Labrie C, Belanger A, Labrie F, Richard D.** Effects of the estrogen antagonist EM-652. HCl on energy balance and lipid metabolism in ovariectomized rats. *Int J Obes Relat Metab Disord* 24: 830–840, 2000.
54. **Pulido R, Zuniga A, Ullrich A.** PTP-SL and STEP protein tyrosine phosphatases regulate the activation of the extracellular signal-regulated kinases ERK1 and ERK2 by association through a kinase interaction motif. *EMBO J* 17: 7337–7350, 1998.
55. **Richards RG, Diaugustine RP, Petrusz P, Clark GC, Sebastian J.** Estradiol stimulates tyrosine phosphorylation of the insulin-like growth factor-1 receptor and insulin receptor substrate-1 in the uterus. *Proc Natl Acad Sci USA* 93: 12002–12007, 1996.
56. **Risinger JI, Maxwell GL, Chandramouli GVR, Jazaeri A, Aprelikova O, Patterson T, Berchuck A, Barrett JC.** Microarray analysis reveals distinct gene expression profiles among histologic types of endometrial cancer. *Cancer Res* 63: 6–11, 2003.
57. **Russell DH, Taylor RL.** Polyamine synthesis and accumulation in the castrated rat uterus after estradiol-17-beta stimulation. *Endocrinology* 88: 1397–1403, 1971.
58. **Salmeeen A, Anderson JN, Myers MP, Tonks NK, Bradford D.** Molecular basis for the dephosphorylation of the activation segment of the insulin receptor by protein tyrosine phosphatase 1B. *Mol Cell* 6: 1401–1412, 2000.
59. **Sato T, Wang G, Hardy MP, Kurita T, Cunha GR, Cooke PS.** Role of systemic and local IGF-1 in the effects of estrogen on growth and epithelial proliferation of mouse uterus. *Endocrinology* 143: 2673–2679, 2002.
60. **Sun H, Charles CH, Lau LF, Tonks NK.** MKP-1 (3CH134), an immediate early gene product, is a dual specificity phosphatase that dephosphorylates MAP kinase in vivo. *Cell* 75: 487–493, 1993.
61. **Takeda-Matsubara Y, Nakagami H, Iwai M, Cui TX, Shiuchi T, Akishita M, Nahmias C, Ito M, Horiuchi M.** Estrogen activates phosphatases and antagonizes growth-promoting effect of angiotensin II. *Hypertension* 39: 41–45, 2002.
62. **Tan YF, Li FX, Piao YS, Sun XY, Wang YL.** Global gene profiling analysis of mouse uterus during the oestrus cycle. *Reproduction* 126: 171–182, 2003.
63. **Tang XM, Rossi MJ, Masterson BJ, Chegini N.** Insulin-like growth factor I (IGF-1), IGF-1 receptors, and IGF binding proteins 1–4 in human uterine tissue: tissue localization and IGF-1 action in endometrial stromal and myometrial smooth muscle cells in vitro. *Biol Reprod* 50: 1113–1125, 1994.
64. **Tanimura S, Nomura K, Ozaki K, Tsujimoto M, Kondo T, Kohno M.** Prolonged nuclear retention of activated extracellular signal-regulated kinase 1/2 is required for hepatocyte growth factor-induced cell motility. *J Biol Chem* 277: 28256–28264, 2002.
65. **Tong W, Pollard JW.** Progesterone inhibits estrogen-induced cyclin D1 and cdk4 nuclear translocation, cyclin E- and cyclin A-cdk2 kinase activation, and cell proliferation in uterine epithelial cells in mice. *Mol Cell Biol* 19: 2251–2264, 1999.
66. **Vairapandi M, Azam N, Balliet AG, Hoffman B, Liebermann DA.** Characterization of MyD118, Gadd45, and proliferating cell nuclear antigen (PCNA) interacting domains. PCNA impedes MyD118 AND Gadd45-mediated negative growth control. *J Biol Chem* 275: 16810–16819, 2000.
68. **Vincent AM, Feldman EL.** Control of cell survival by IGF signaling pathways. *Growth Horm IGF Res* 12: 193–197, 2002.
69. **Warrington JA, Nair A, Mahadevappa M, Tsyganskaya M.** Comparison of human adult and fetal expression and identification of 535 housekeeping/maintenance genes. *Physiol Genomics* 2: 143–147, 2000.
70. **Watanabe H, Suzuki A, Kobashi M, Takahashi E, Itamoto M, Lubahn DB, Handa H, Iguchi T.** Analysis of temporal changes in the expression of estrogen-regulated genes in the uterus. *J Mol Endocrinol* 30: 347–358, 2003.
71. **Weihua Z, Ekman J, Almkvist A, Saji S, Wang L, Warner M, Gustafsson JA.** Involvement of androgen receptor in 17beta-estradiol-induced cell proliferation in rat uterus. *Biol Reprod* 67: 616–623, 2002.
72. **Wing LY.** Effect of estradiol on the activities of ornithine decarboxylase and S-adenosyl-methionine decarboxylase in tissues of ovariectomized rats. *Chin J Physiol* 31: 95–103, 1988.
73. **Zhang ZY.** Protein tyrosine phosphatases: prospects for therapeutics. *Curr Opin Chem Biol* 5: 416–423, 2001.
74. **Zhang ZY, Zhou B, Xie L.** Modulation of protein kinase signaling by protein phosphatases and inhibitors. *Pharmacol Ther* 93: 307–317, 2002.